

*Original Research*

# Assessing the Variation of Glaciers Velocity in Hunza Basin, Gilgit Baltistan Using Advanced Geospatial Techniques

**Shahid Iqbal\*, Sajid Rashid Ahmad**

College of Earth and Environmental Sciences, University of the Punjab, Lahore 54590, Pakistan

*Received: 25 September 2022*

*Accepted: 16 January 2023*

## Abstract

World's largest glaciers lie in Hindu Kush Himalayan (HKH) outside polar region, are the source of fresh water which accommodates the needs of millions of people living downstream. Impact of changing climate on cryosphere can be measured critically from glacier movement due to global warming. Due to complex terrain and unpredictable weather, it is not feasible to measure glaciers' velocity and movement through field surveys physically. For this purpose, the current study aimed to assess the variation of glaciers velocity using advance geospatial technique like the co-registration and correlation (COSI-CORR) of optically sensed satellite images. Time-series analysis on the Landsat-8 data (2013–2020) revealed successfully for computing the surface ice velocity of glaciers of Hunza Basin. Results show that the velocity of a glacier increases with the altitude whereas speed decreases at the terminus. Moreover, it has been noted from spatial patterns of glacier surface ice velocity that the tributary glaciers contribute to the mainstream glacier velocity significantly, which increases at the terminus. Subsequently, the varying ice velocity was determined by orientation, debris cover, glacier size, and altitude for glaciers. The study recommended to regularly monitor the dynamics of glaciers in this region to cater the impacts of global warming and climate change.

**Keywords:** glacier velocity, climate change, Hunza basin, COSI-CORR

## Introduction

For mapping the glaciers ice on a global scale for hazard management and glacier flow, a number of optical satellites are operated for covering Earth's surface globally. The glacier velocity is a function of bed deformation, glacier sliding, and ice deformation sliding [1-5]. In cryosphere, glacier velocity plays

a vital role because it's all about the mass balance because by glacier movement the mass gathered at top is shifted downwards [3, 6]. The mechanism of debris transfer can be easily determined by glacier velocity [1, 7-8], which dictates the glacier's bear capacity [9] and stability condition for hazard monitoring [6, 10]. The status of glaciers' fitness can be estimated through glacier velocity on regular basis [3, 7, 9, 11]. Similarly, the dynamic behavior of Himalayan debris-covered glaciers is well determined by the glacier velocity instead of mass balance data (because of limited availability) [1, 7, 12]. It is relatively simple to find glacier velocity

---

\*e-mail: shahidiqbal0506@gmail.com

from remote sensing data rather the physical survey and instrument [3]. For last few decades, the change in Himalayan glaciers has been under discussion [13-16], however, some studies explored extensive retreat and shrinkage of glaciers during the last century [7, 17]. In the Himalayas, the deceleration of glaciers has been reported due to down mass wasting [1, 3, 18-20]. However, some authors understanding about the glacier movement is limited because of sparse glacier velocity measurements [3, 4, 7, 11]. It was reported that 94% of glacier velocity variations are controlled by ice thickness change at the regional level [3].

Multiple methods are available to monitor and measure the surface glacier velocities like SAR feature tracking technique [21-22], interferometry of SAR imagery [23-24], and cross-correlation of optical imagery [12, 25-27]. Many studies are conducted using SAR datasets as well as optical data. InSAR and DInSAR techniques are commonly used, while dealing with SAR datasets for estimation of glacier velocity [28] but it has few limitations for highly complex terrains like Hindu Kush and Himalayan regions [29]. High accuracy and few centimeters per year precision can be achieved with these feature tracking methods that required better coherence between the image pairs, which is sometimes difficult to find because of changing glacier features [30-31]. Hence, velocity derived from interferometry technique may be illustrative for short-term observations and it is difficult to extrapolate in terms of annual velocity [30]. Cross-correlation of optical imagery is similar to offset tracking of SAR by using coherence or intensity of SAR images [32-33]. Feature tracking method of SAR is more suitable for estimating glacier velocities for long periods as compared to the interferometry technique [34]. In recent decades, the optical image correlation technique for measuring displacement of features in earth and geological science has been widely used. In the feature tracking method, two images are correlated to measure displacement and one image is treated as a master image whereas the other is a slave [11, 35]. In this technique, a matrix is selected on the master image with some center and the same window is dug out from the slave image and both are compared using similar function. The same scenario is applied to the whole image to measure the displacement of pixels by interpolation [26]. Till 1980, feature tracking was carried out manually for two images of different times, which was time taking and less accurate. The accuracy and detail of measurement depend on the precision of two co-registered images and the resolution of the sensor [12, 36]. First automated cryospheric feature tracking was carried out by [37], based on normalized cross-correlation (NCC) algorithms with more accurate results. The comparison method can be based on underlying features or an area. The first type (NCC) mined out features in pre-processing phase from the image whereas in the later method image quantities are compared. For cryospheric studies, the correlation window size is significant.

Mostly large window size is recommended to cater all the differences in digital numbers (DN) and filter out noise. In case of a small window size, the size should be very small so that distortions within the window can be ignored. The correlation window size differs for the glacier to glacier subject to glacier aspect and contrast.

Some researchers around the globe observed the thinning and retreat of some glaciers existing in the HKH region and the glaciers in Upper Indus Basin (UIB) are also experiencing changes and shrinking [14, 20, 38-40]. The mean maximum temperature of northern areas increased from 1989 to 2018 [41]. The air temperature in the Liddar valley has also increased during 1962-2010. Some regions of the Himalayas are warming at a higher rate [42]. While inspecting temperature variations in the Himalayas, [43] informed a increase of 1.6°C from 1901 to 2002. According to [44], due to a rise in temperature the process of glacier melting increases. [45] also stated a firm increase in temperatures (maximum and minimum) at two meteorological stations near the Hispar glacier. Due to climate change and global warming, Pakistan is facing a rise in temperature of 0.76°C over the last 40 years, and on the other hand this increase in temperature was significantly higher i.e., 1.5°C during the same period in high altitude mountainous regions [46]. A rise in temperature 25.82°C to 26.74°C from 1988 to 2017 observed for Mansehra [47]. The current study is intended to measure the variation of glaciers velocity in Hunza Basin using advance geospatial techniques on Landsat 8 time series data. No such study has been conducted so far on the upper Indus basin (UIB) to measure the variation of glaciers velocity using adopted techniques. This study is very important to monitor the glaciers health and assess the variation of glaciers velocity with respect to changing climate in Pakistan. Recent mighty floods in northern regions caused a lot of damage and devastated the country economy badly. Studied glaciers in this study also contributed to a larger extent in causing these floods. Therefore, it becomes a need of the hour that behavior and impact of climate on these glaciers must be examined in a careful way in order to mitigate such challenges in future. The policy makers, food security (FAO), water regulating and power generating authorities like International Water Management Institute (IWMI), Pakistan Meteorological Department (PMD) and Water and Power Development Authority (WAPDA). Novelty is so far no such study has been conducted in Pakistan where this advanced technique has been practiced. Some studies have conducted in this region used traditional and obsolete methods which involve huge resources and time.

## Materials and Methods

The study was carried out on Hunza basin, which lies in Hindu Kush-Himalaya (HKH) region and is one

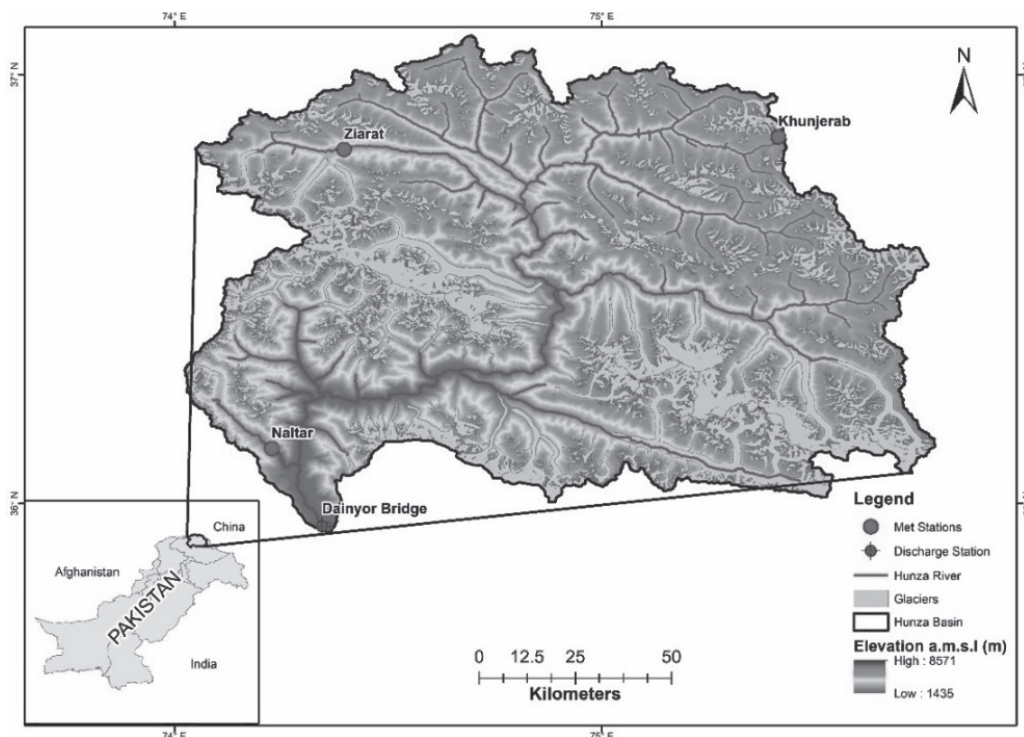


Fig. 1. Location Map of Hunza Basin.

of the sub-basins of the Upper Indus Basin (Fig. 1). The spatial extent of Hunza basin ranges between 35°55' to 37°06'N latitudes, 74°03' to 75°49'E longitudes and covers an area of about 13,559 km<sup>2</sup> with an average elevation of 4,655 m. Hunza basin is unique because of a large number of high elevated glaciers including, Batura, Hispar, Khurdopin, Momhil, Mulungutti, Virjerab and Yazgil.

The main source of data was Landsat 8 (OLI) obtained from USGS website (<http://earthexplorer.usgs.gov/>). Digital Elevation Model (DEM) with a spatial resolution of 30 m was downloaded from <https://www.eorc.jaxa.jp/ALOS/en/aw3d30/data/index.htm>. All images having minimum cloud cover (i.e., <10%) were downloaded for 2013-2020 (Table 1),

preprocessed and projected into WGS84 and UTM zone 43 projection, using ENVI, Erdas Imagine and ArcGIS.

There are about 20 meteorological stations in the upper Indus basin, functioned by Pakistan meteorological department (PMD) and Water and Power Development Authority (WAPDA). For the current study, daily minimum temperature, maximum temperature and precipitation data were obtained from following stations Khunjerab, Ziarat and Naltar operated by WAPDA (Table 2).

For the correlation of optical images, different techniques have been applied and developed like normalized cross-correlation [48-49], phase correlation [50], least-squares [51], and orientation correlation (CCF-O) [52]. It has been stated that phase correlation

Table 1. List of Input Datasets Used for Current Study.

Objective	Platform & Sensor	Spatial Resolution	Date of acquisition
Surface Ice Velocity	Landsat 8- OLI	15 m	2013-10-09
Surface Ice Velocity	Landsat 8- OLI	15 m	2014-07-24
Surface Ice Velocity	Landsat 8- OLI	15 m	2015-09-13
Surface Ice Velocity	Landsat 8- OLI	15 m	2016-10-01
Surface Ice Velocity	Landsat 8- OLI	15 m	2017-08-01
Surface Ice Velocity	Landsat 8- OLI	15 m	2018-08-04
Surface Ice Velocity	Landsat 8- OLI	15 m	2019-09-24
Surface Ice Velocity	Landsat 8- OLI	15 m	2020-04-19
Slope, Aspect	SRTM DEM-v3	30 m	2000-02-30

Table 2. Meteorological Data of Hunza Basin Stations from 1995-2018.

Stations	Elevation m.a.s.l	T <sub>max</sub> °C	T <sub>min</sub> °C	T <sub>s</sub> °C	T <sub>w</sub> °C	P mm/yr
Khunjerab	4730	-0.88	-10.97	6.43	-13.44	202.21
Ziarat	3699	6.56	-2.65	9.46	-4.06	228.59
Naltar	2810	10.01	1.403	13.78	-1.01	648.89

and orientation correlation exist in COSI-Corr are comparatively more vigorous methods for monitoring glacier velocities on global scale [11]. For this purpose, there are few open-source software available like IMGRAFT, IMCORR, CIAS, COSI-Corr, etc. But, the tool which performed better was COSI-Corr [53] with some add-on advantages like pre and post-processing [54]. In this study for measuring glacier velocity, COSI-Corr tool (ENVI software module) was used with more precise co-registration, sub-pixel correlation, and ortho-rectification of optical images. The cross-correlation algorithm is the foundation of feature tracking which figures out the highest correlation offsets on temporal satellite datasets. One image is treated as a master and the other as a slave for comparison where correlation is the grade of similarity. The equation for cross-correlation is:

$$CC(u, v) = \frac{\sum_{x,y} (f(x,y) - \bar{f})(g(x+u, y+v) - \bar{g})}{\sqrt{\sum_{x,y} (f(x,y) - \bar{f})^2 \sum_{x,y} (g(x+u, y+v) - \bar{g})^2}} \quad (1)$$

Where  $f(x,y)$  and  $g(x,y)$  are the pixel values in correlation windows of two images, offsets between two windows are denoted by  $u$  and  $v$ ,  $\bar{f}$  and  $\bar{g}$  ( $u,v$ ) are the average pixel values of correlation windows. The size of correlating window is large enough to cater all potential changes in terms of displacement [55]. According to the literature, the size of window should be at least twice than the projected displacements. To get accurate results, the filed base knowledge of displacement size should be known for appropriate adjustment of values which in the current scenario are not available. The "Correlation" function compares both images and generates a relative displacement map. There are two images one for pre-event and the other for post-event. The first image has been treated as a master or reference image and the other as a slave image where displacements can be measured as compared to the reference one. This produces output in three bands: (1) displacement in the East-West direction (2) displacement in the North-South direction and (3) signal-to-noise ratio (SNR) resulting in a displacement field. The signal-to-noise ratio is used to measure the quality of correlation between the pair of two images. While processing, the small errors at each stage lead to a higher error of final output [12, 56] but these can be minimized by using built-in filtering algorithms of COSI-Corr [54].

Two options were there for calculating the correlation of images in ENVI software: i.e., frequential

domain and the other is the statistical domain. The results obtained from the frequential correlation are much more precise than the other one because it is based on Fourier operations [54]. The frequency correlation is sensitive to noise therefore, it is suggested for image pair with fine spatial resolution. On the other hand, statistical correlation is coarser and the value of the absolute correlation coefficient is maximum. Thus, recommended for the correlation of noisy image pairs. In the present study, the frequency correlation method was used which requires several initial parameters: window size, step size, robustness iteration and mask threshold.

To get better results both images were geo-referenced and mapped to the same projection having a finer spatial resolution for correlation i.e., panchromatic. According to [57], the resolution of data is directly proportional to glacier velocity feature extraction. Based on different experimental studies, a window size of 64 x 32 pixels and 128 x 32 pixels showed good results for slow-moving ice [12]. Here, the window size of 128 x 32 pixels and step size of 16 x 16 pixels have been selected. To get better accuracy of correlation results and reduce the impact of noise, the frequency mask threshold of 0.9 and robustness iteration of 2 was set. For calculation of velocity, both displacement layers (north-south and east-west) were exported as separate files and filtered low SNR values to minimize the noise of the surrounding. The resolution of resultant displacement vector is determined by the 16 x 16 pixels step size. The result is then normalized to 365 days (i.e., a year) to get displacement in meters per year, and uncertainty factor is also incorporated (Fig. 2).

Limited studies were conducted while using cross-correlation of images from Landsat on the displacement error field sources [56-58]. It was comprehensively reported that velocity/ displacement field errors of Landsat 8 were caused mainly by satellite artifacts, wavelength orbital error, topographic artifacts, temporal decorrelation noises, and attitude jitter distortions [56]. These errors can be removed by using a longer period between pairs of images. The accuracy of final velocity products was estimated by the quality of the dataset used which depends on gradient, direction, and magnitude [12]. The off- glacier observed velocities error was calculated by the formula [49]:

$$\sigma_{\text{off}} = \sqrt{SE^2 + MEAN^2} \quad (2)$$

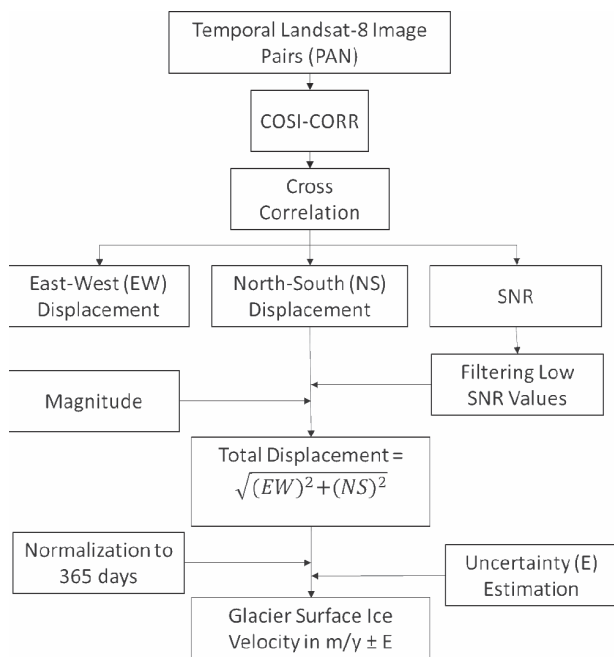


Fig. 2. Detailed Methodology flow diagram.

In current study, 1000 random points were derived, which shows mean displacement of <5 m for the stable terrain (Online resource).

### Results

The resultant annual-mean glacier velocities of seven major glaciers of Hunza Basin were measured

using the COSI-CORR tool of ENVI software, applied on Landsat 8 (OLI) panchromatic images during 2013-2020, and were tabulated in Table 1. Glacial behavior is affected by varying precipitation and temperature. Results revealed that during 2016, all glaciers show a decreasing velocity trend except for the Batura glacier, while the Yagzil glacier surged with the highest velocity of 103.21 myr<sup>-1</sup> during 2019. However, the Hispar glacier advanced with the least velocity of 3.62 myr<sup>-1</sup> in 2018. All the glaciers of Hunza Basin except Batura showed decreasing velocity pattern in 2016. Maximum decreasing velocity (59.74 myr<sup>-1</sup>) was noticed against the Momhil glacier in 2016, while minimum (5.19 myr<sup>-1</sup>) for Batura glacier in 2018. Maximum average annual velocity was observed against Yazgil glacier (50.55 myr<sup>-1</sup>), whereas minimum average annual velocity against Hispar glacier (30.25 myr<sup>-1</sup>) was observed. The glacier velocity other than the maximum value is characterized by gradual changes in the slope. In addition to climatic factors, it is also controlled by topographic factors.

Results revealed that glacier velocity of Batura glacier rises from 2014 to 2015, then decreases till 2018 and in 2019 glacier velocity increased by 20.66%. The fluctuating trend of the Batura glacier indicates that its annual-mean velocity was reported with a decreasing value at a rate of 16.67% per annum with an average annual velocity of 42.60 myr<sup>-1</sup>. The glacier velocity is maximum at 3,340 m.a.s.l. which gradually decreases downward (Fig. 3).

Fig. 4 shows that the velocity of Hispar glacier has also been increasing from 2014 to 2015, followed by decreasing and increasing trend, the glacier velocity

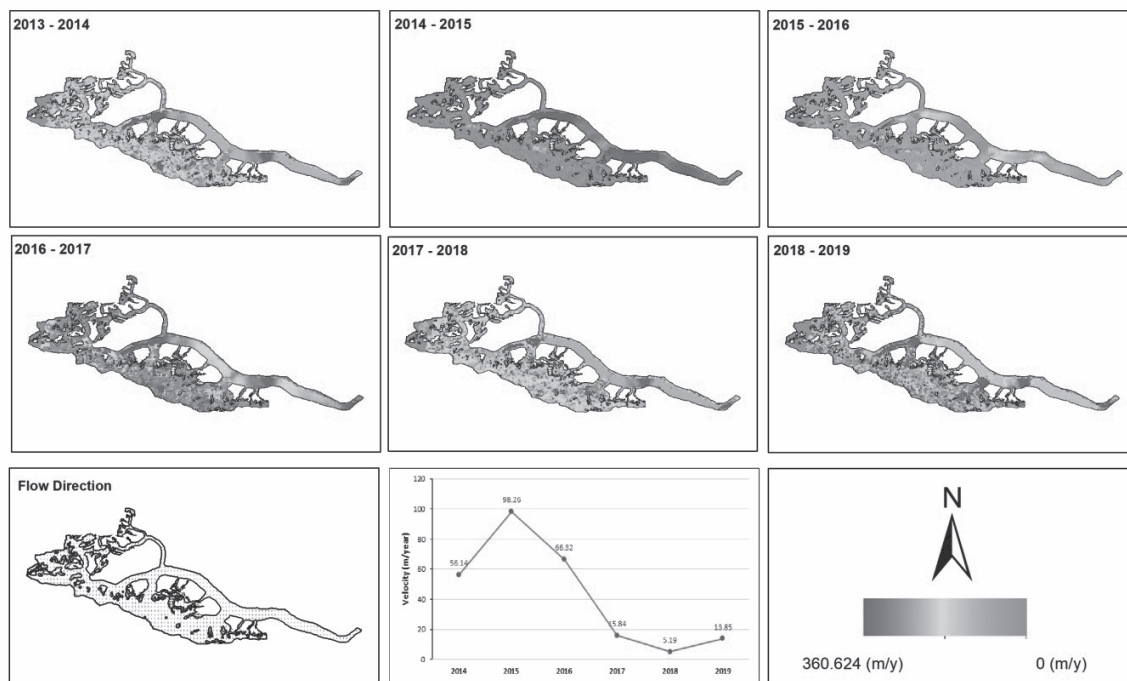


Fig. 3. Batura Glacier Velocity Trend.

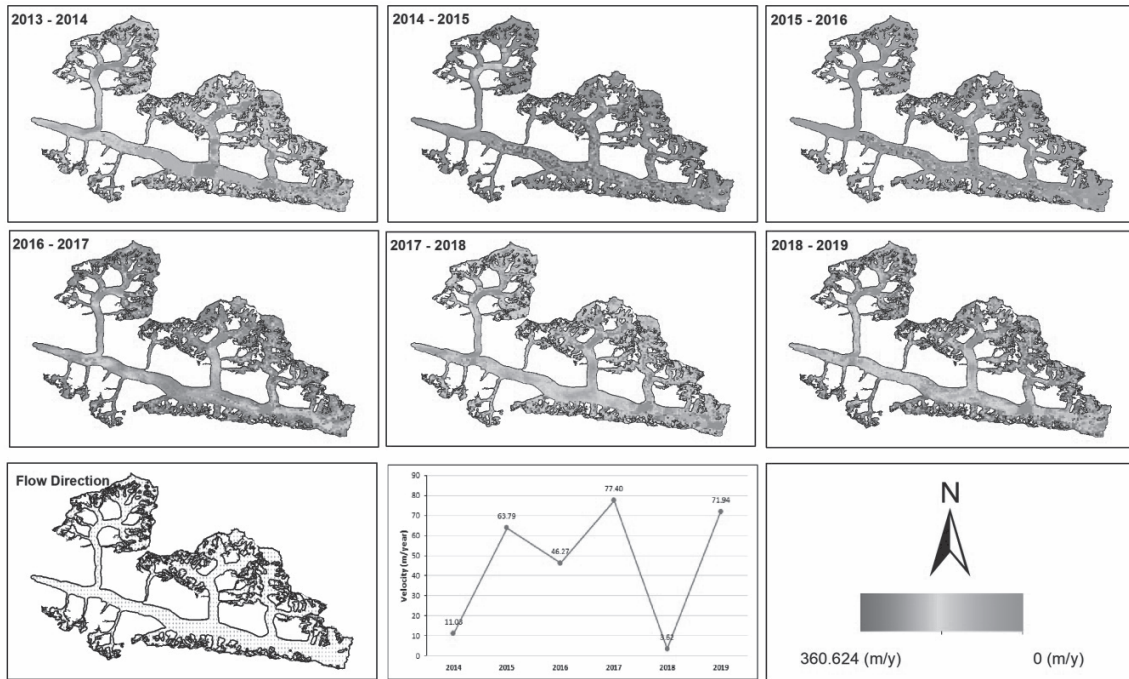


Fig. 4. Hispar Glacier Velocity Trend.

again increased in 2019. Whereas, annual-mean velocity variational pattern is sinusoidal, with peak value  $77.40 \text{ myr}^{-1}$  in 2017, while minimum ( $46.27 \text{ myr}^{-1}$ ) in 2016. The varying trend of Hispar glacier indicates that its annual-mean velocity has been increasing at a rate of 12.30% per annum with an average annual velocity of  $45.68 \text{ myr}^{-1}$ . The glacier velocity is maximum above 3,500 m a.s.l. which gradually decreases downward.

Fig. 5 represents the velocity distribution of Khurdopin glacier. The glacier velocity increases from 2014 to 2015, then decreases in 2016 and increases till 2019. The annual-mean velocity variational pattern is sinusoidal, with a peak value ( $93.36 \text{ myr}^{-1}$ ) in 2019, while minimum ( $39.39 \text{ myr}^{-1}$ ) in 2016. The changing pattern of Khurdopin glacier indicated that annual-mean velocity has been increasing at a rate of 11.87%

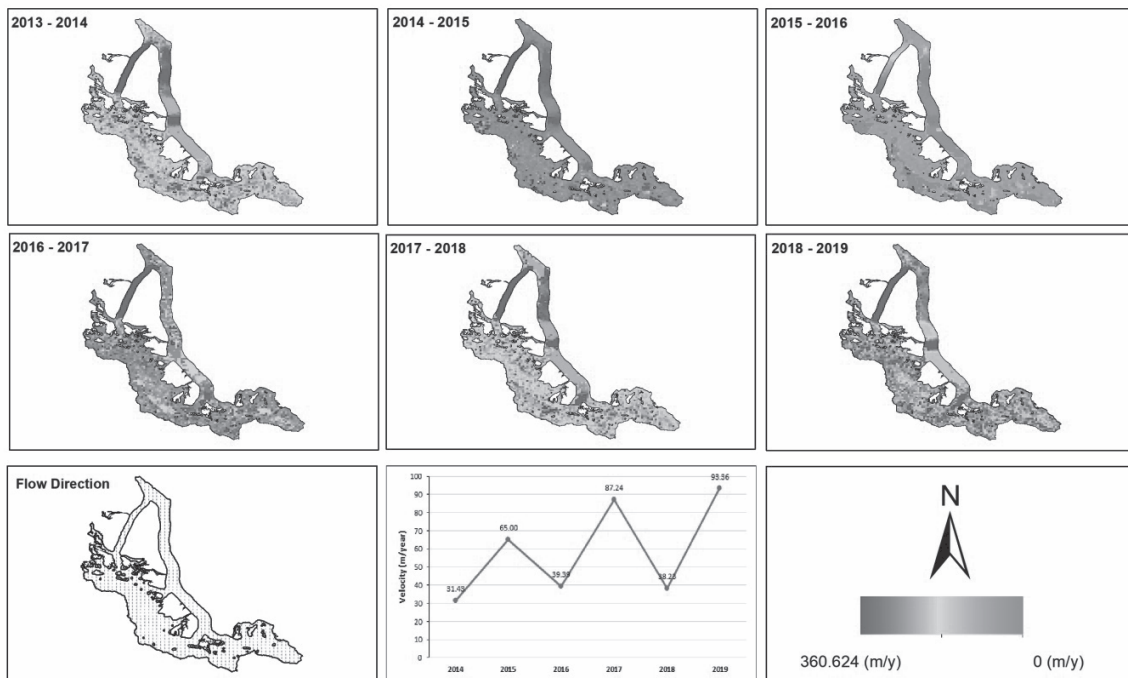


Fig. 5. Khurdopin Glacier Velocity Trend.

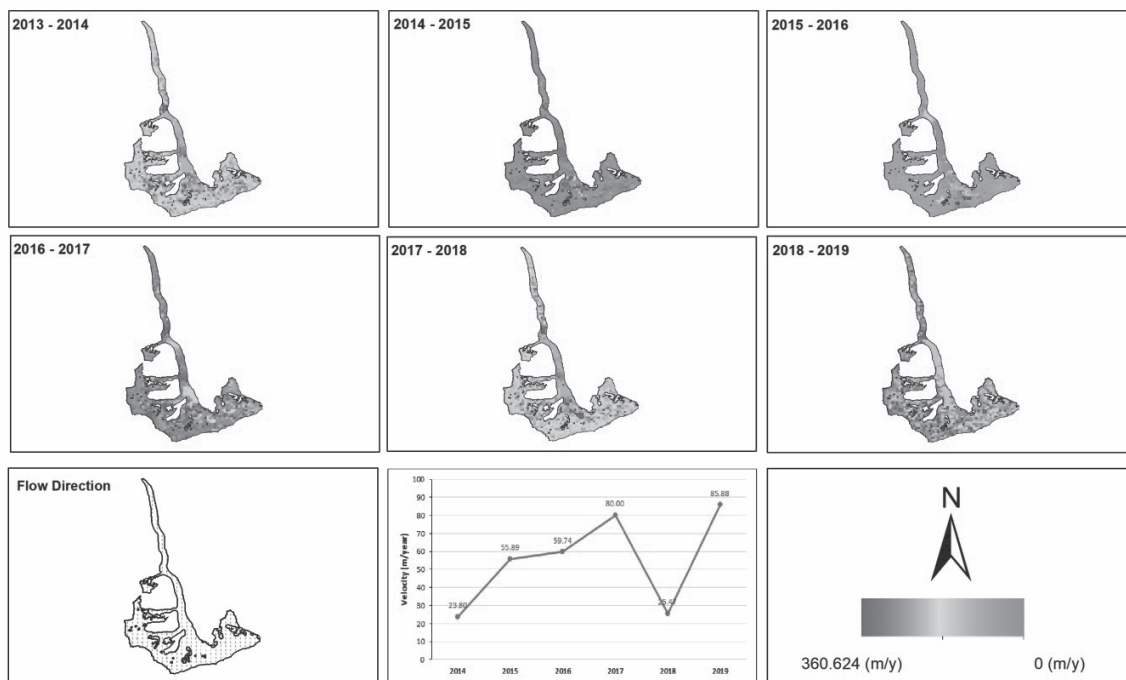


Fig. 6. Momhil Glacier Velocity Trend.

per annum during with an average annual velocity of 49.11 myr<sup>-1</sup>.

For Momhil glacier, overall glacier movement increased with the maximum value varying from 59.74 myr<sup>-1</sup> to 85.88 myr<sup>-1</sup>. The observed annual-mean velocity variational pattern was sinusoidal, with peak value (85.88 myr<sup>-1</sup>) in 2019, while minimum (59.74 myr<sup>-1</sup>) in 2016. The Momhil glacier altering behaviour indicated that the annual-mean velocity

has been increasing at a rate of 14.04% per annum with an average annual velocity of 55.13 myr<sup>-1</sup>. The glacier velocity is maximum above 3,500 m.a.s.l which gradually decreases downstream (Fig. 6).

Fig. 7 shows that the velocity of Mulungutti glacier has also been increasing from 2014 to 2015, 2017 and 2019. The annual-mean velocity variational pattern is sinusoidal, with a peak value (97.54 myr<sup>-1</sup>) in 2019, while minimum (59.41 myr<sup>-1</sup>) in 2016. The fluctuating

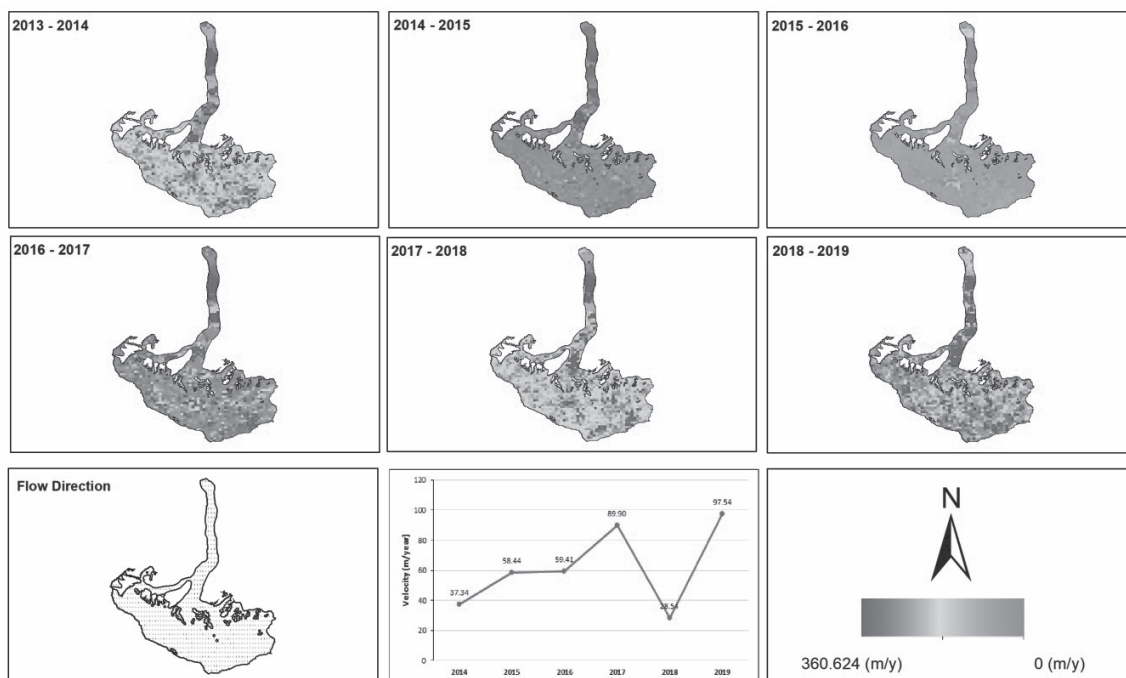


Fig. 7. Mulungutti Glacier Velocity Trend.

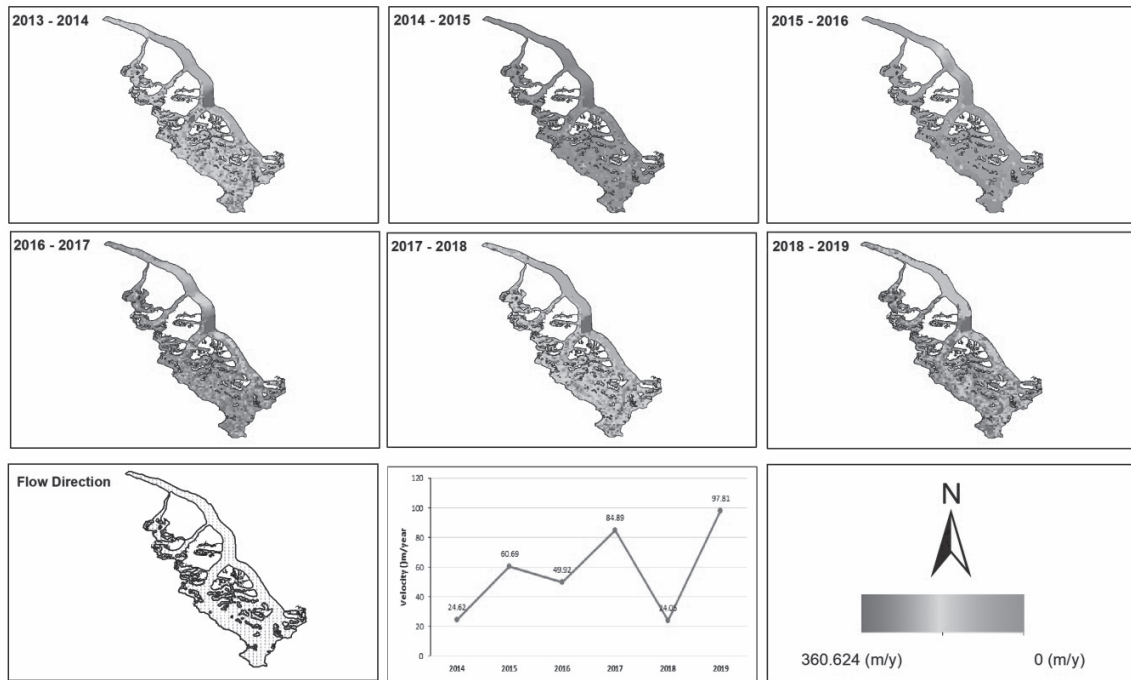


Fig. 8. Virjerab Glacier Velocity Trend.

pattern of Mulungutti glacier indicates that its annual-mean velocity has been increasing at a rate of 12.66% per annum during the study year with an average annual velocity of 61.86 myr<sup>-1</sup>.

Fig. 8 shows the velocity distribution of Virjerab glacier. The velocity significantly increases from 24.62 myr<sup>-1</sup> to 84.89 myr<sup>-1</sup>. The irregular trend of Virjerab glacier indicates that its annual-mean velocity

has been increasing at a rate of 13.63% per annum during the study year with an average annual velocity of 57.00 myr<sup>-1</sup>. The glacier velocity is maximum above 5,000 m.a.s.l. which gradually decreases downward.

For Yazgil glacier, overall glacier velocity increased with the maximum value changing from 42.83 myr<sup>-1</sup> to 103.21 myr<sup>-1</sup> (Fig. 9). The peak in glacier velocity occurred at approximately 5,000 m.a.s.l. The annual-

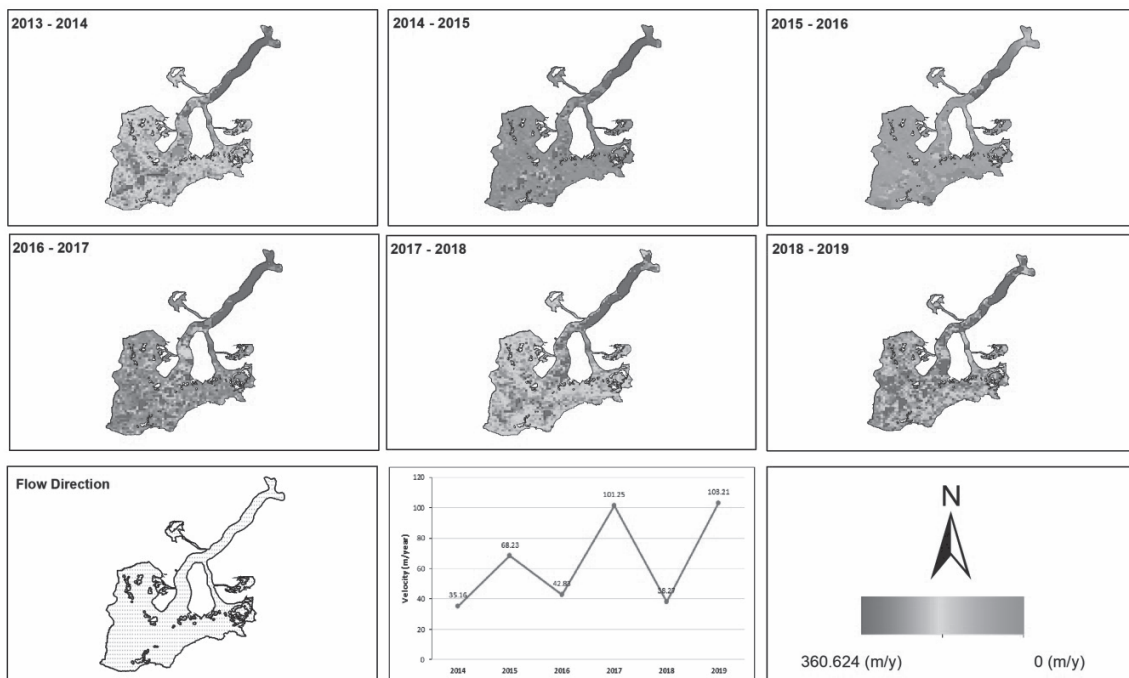


Fig. 9. Yazgil glacier Velocity Trend.

Table 3. Annual-mean glacier velocities ( $\text{myr}^{-1}$ ) in Hunza Basin during 2014 – 2019.

Year	Batura Glacier	Hispar Glacier	Khurdopin Glacier	Momhil Glacier	Mulungutti Glacier	Virjerab Glacier	Yazgil Glacier
2014	56.14	11.03	31.43	23.80	37.34	24.62	35.16
2015	98.26	63.79	65.00	55.89	58.44	60.69	68.23
2016	66.32	46.27	39.39	59.74	59.41	49.92	42.83
2017	15.84	77.40	87.24	80.00	89.90	84.89	101.25
2018	5.19	3.62	38.23	25.47	28.54	24.05	38.27
2019	13.85	71.94	93.36	85.88	97.54	97.81	103.21
Average Velocity	42.60	45.68	59.11	55.13	61.86	57.00	64.83

mean velocity variational pattern is sinusoidal, with a peak value ( $103.21 \text{ myr}^{-1}$ ) in 2019, while minimum ( $42.83 \text{ myr}^{-1}$ ) in 2016. The varying behaviour of Yazgil glacier reflected that its annual-mean velocity has been increased at a rate of 11.93% per annum with an average annual velocity of  $64.83 \text{ myr}^{-1}$ .

Cumulative results of major glaciers of Hunza Basin are summarized in Table 2 and their fluctuating trend from 2013-2020 is shown in Fig. 10. Whereas, the cumulative surface velocity map of these glaciers is shown in Fig. 11.

### Discussions

In this research the variation of glaciers velocity has been investigated in the Hunza basin (Batura, Hispar, Khurdopin, Momhil, Mulungutti, Virjerab and Yazgil) using Landsat multitemporal panchromatic images from 2013 to 2020. Results of this research have been found consistent with following studies: [59] reported the increasing surface velocity of Pasu glacier from 1993-2019. Due to negative mass balance of Maritime glacier of Kangri Karpo mountains decreased during 1988-2017 [60]. A study was conducted to monitor the glacier velocity variation over recent decades from six regions using satellite imagery, and show that due to

negative mass balance their velocities decreased [11]. The consistent slowdown of 9 out of 11 glaciers with ice thinning in High Mountain Asia was observed [3]. Analysis to assess the change in glacier at regional scale permits to discover the effect of climate forcing on glaciers usually it has been found that seasonal changes. [61] reported the reduction of glacier thickness and slow down of 18 central Himalayan glaciers of India. Studies also showed that the average mass balance of ice caps and glaciers globally are negative, mainly the glaciers of central Himalaya with negative values [62-63]. The Results of the study are in line with the glacier velocities and positive mass balance as examined by [3]. [64] measured the stability of Batura glacier using Karakoram Anomaly in 2017. The surface velocities of seven major glaciers in Hunza basin are heterogeneous because it depends on altitude, slope, mass balance, sensitive to temperature and size of glacier [3-4, 61, 65]. Past studies have revealed that, glaciers flow much faster when melting occurs in summer with strong spatial and temporal variations [66-68]. Moreover it has been observed that the conflicting difference between eastern and western parts of the Himalaya, representing heterogeneous change in melting and accumulation under diverse climatic regimes. Change in velocity is small during winter.

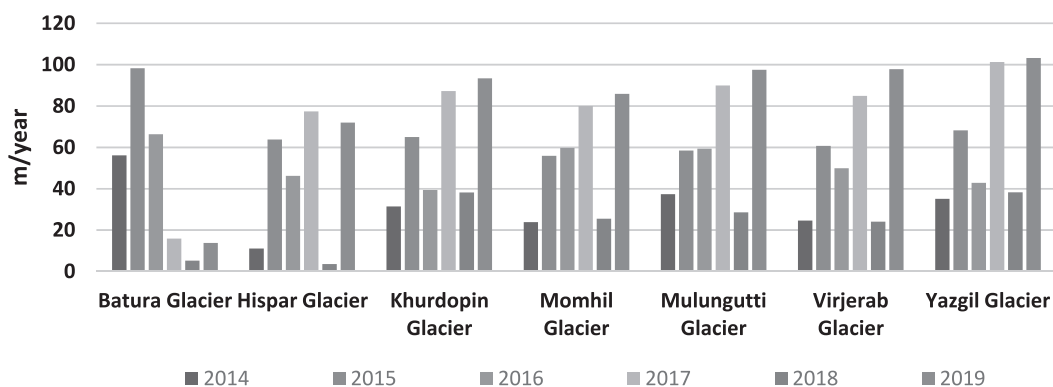


Fig. 10. Glacier Velocity during 2014-2020.

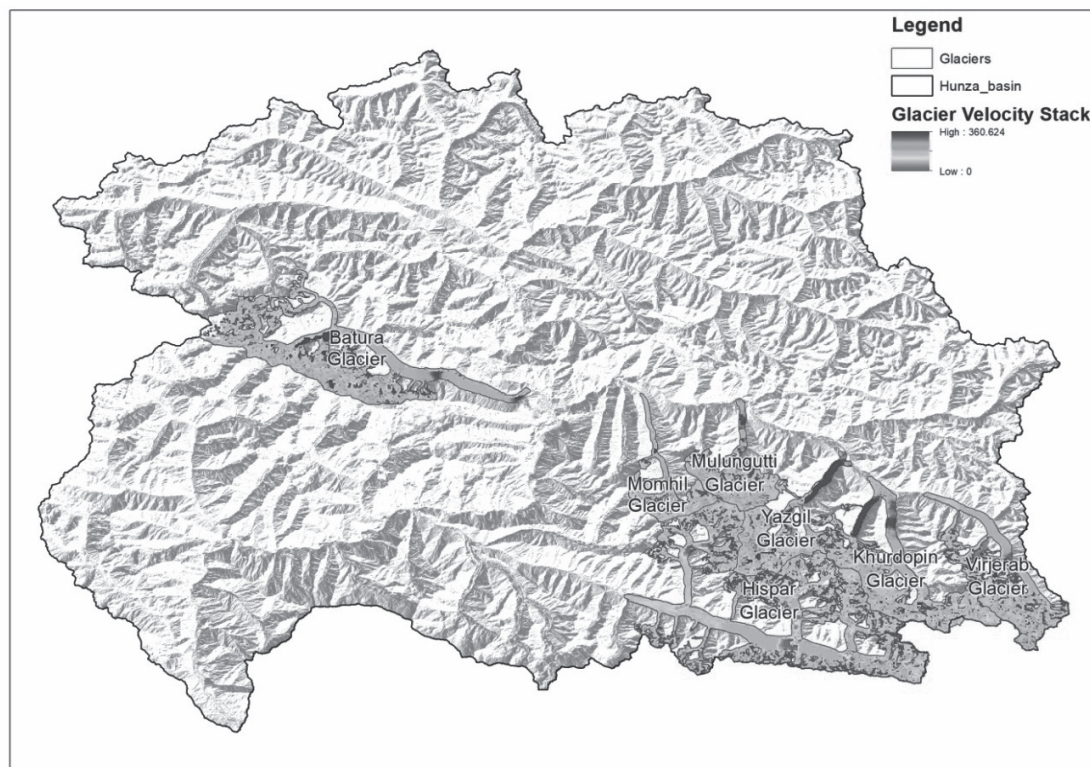


Fig. 11. Stack velocity of the seven major glaciers in Hunza Basin from 2013-2020.

The glaciers of study area are relatively stable as compared to other regions of the globe whereas the behavior of glaciers below 5000 m.a.s.l. changes significantly. These results were also validated indirectly from the water discharge data of glaciers provided by WAPDA and PMD. It was evident from Fig. 11 that the glacier velocity is highest along the main stream from the terminus which gradually decreases with elevation for accumulation area and increases with elevation for ablation area. Advance Geospatial techniques are found quite helpful in achieving the desired results in line and consistent with following studies [69-95] for assessing the variation of glaciers velocity. As an outcome of this research decision makers will be in a better position to devise a plan for food security, water regulating and power generating authorities keeping in mind the climate change and global warming. Meanwhile no *in-situ* data available yet for monitoring glacier health and their properties for current basin, however uncertainties should not be overlooked because of the varying behavior of glaciers due to local dynamics of the basin which may not be identified using remote sensing data only.

### Conclusions

In the current study, the glacier velocity was successfully investigated by COSI-CORR method on panchromatic Landsat-8 (OLI) imagery. This research

analyzed the patterns of individual glacier and found that glacier velocity exhibits heterogeneity at different temporal and spatial scales which varied for the low elevation regions with slightly higher velocity. This was validated indirectly from river discharge data and as well as from past literature. The extension COSI-CORR is freely available for scientific community. It is more efficient for determining minor displacement movements using feature tracking on high resolution data. This study shows that COSI-CORR method can be used on high resolution panchromatic imagery data to determine the glacier movements with respect to static or non-glacial objects for assessing the variation of glaciers velocity. The glacier velocities exhibited prominent differences regionally. The glacier velocity increases beyond 5000 m a.s.l. approximately which gradually decreases onwards which is evident spatially from the figures of individual glacier velocities. Due to different topographic features like slope, aspect and elevation of these glaciers, the velocity varies. The present study determined that for glacial retreating one of the main factors is warmer temperature, as temperature increases the glaciers melt more rapidly than progression. Besides, changing climate is also impacting the ice reserves globally. The glacier velocity may have short-term and long-term implications. Glacier velocity is the sum of ice deformation and basal sliding. Hence the current study hereby proposed consistent checking of climatic impacts in terms of glacier dynamics and their possible hazards.

### Acknowledgments

We also express our gratitude to the kind responses of Water and Power Development Authority of Pakistan (WAPDA) and Pakistan Meteorological department (PMD) for providing ground data. We express our sincere thanks to friends and fellows, for their kind advice and moral support.

### Conflict of Interest

The authors declare no conflict of interest.

### References

1. RACOVITEANU A.E., NICHOLSON L., GLASSER N.F., MILES E., HARRISON S., REYNOLDS J.M. Debris-covered glacier systems and associated glacial lake outburst flood hazards: challenges and prospects. *Journal of the Geological Society*, **179** (3), **2022**.
2. HEWITT K. Glaciers of the Karakoram Himalaya. *Encyclopedia of snow, ice and glaciers*, 429, **2014**.
3. DEHECQ A., GOURMELEN N., GARDNER A.S., BRUN F., GOLDBERG D., NIENOW P.W., TROUVÉ E. Twenty-first century glacier slowdown driven by mass loss in High Mountain Asia. *Nature Geoscience*, **12** (1), 22, **2019**.
4. GARG P.K., SHUKLA A., TIWARI R.K., JASROTIA A.S. Assessing the status of glaciers in part of the Chandra basin, Himachal Himalaya: a multiparametric approach. *Geomorphology*, **284**, 99, **2017**.
5. HEID T. Deriving glacier surface velocities from repeat optical images, **2011**.
6. MOUGINOT J., RIGNOT E., SCHEUCHL B. Continent-wide, interferometric SAR phase, mapping of Antarctic ice velocity. *Geophysical Research Letters*, **46** (16), 9710, **2019**.
7. SHUKLA A., QADIR J. Differential response of glaciers with varying debris cover extent: evidence from changing glacier parameters. *International Journal of Remote Sensing*, **37** (11), 2453, **2016**.
8. JONES D.B., HARRISON S., ANDERSON K. Mountain glacier-to-rock glacier transition. *Global and Planetary Change*, **181**, 102999, **2019**.
9. TIWARI R., GUPTA R., ARORA M.K. Estimation of surface ice velocity of Chhota-Shigri glacier using sub-pixel ASTER image correlation. *Current Science*, 853, **2014**.
10. WANG W., XIANG Y., GAO Y., LU A., YAO, T. Rapid expansion of glacial lakes caused by climate and glacier retreat in the Central Himalayas. *Hydrological Processes*, **29** (6), 859, **2015**.
11. HEID T., KÄÄB A. Evaluation of existing image matching methods for deriving glacier surface displacements globally from optical satellite imagery. *Remote Sensing of Environment*, **118**, 339, **2012**.
12. VECCHIO A.L., LENZANO M.G., DURAND M., LANNUTTI E., BRUCE R., LENZANO L. Estimation of surface flow speed and ice surface temperature from optical satellite imagery at Viedma glacier, Argentina. *Global and planetary change*, 169, 202, **2018**.
13. COGLEY J.G., KARGEL J.S., KASER G., VAN DER VEEN C.J. Tracking the source of glacier misinformation. *Science*, **327** (5965), 522, **2010**.
14. KULKARNI A.V., KARYAKARTE Y. Observed changes in Himalayan glaciers. *Current Science*, 237, **2014**.
15. NEGI H.S., SARAVANA G., ROUT R., SNEHMANI. Monitoring of great Himalayan glaciers in Patsio region, India using remote sensing and climatic observations. *Current Science*, 1383, **2013**.
16. RANKL M., KIENHOLZ C., BRAUN M. Glacier changes in the Karakoram region mapped by multitemporal satellite imagery. *The Cryosphere*, **8** (3), 977, **2014**.
17. BRUN F., BERTHIER E., WAGNON P., KÄÄB A., TREICHLER D. A spatially resolved estimate of High Mountain Asia glacier mass balances from 2000 to 2016. *Nature Geoscience*, **10** (9), 668, **2017**.
18. DAVAZE L., RABATEL A., DUFOUR A., HUGONNET R., ARNAUD Y. Region-wide annual glacier surface mass balance for the European Alps from 2000 to 2016. *Frontiers in Earth Science*, **8**, 149, **2020**.
19. BONEKAMP P.N., DE KOK R.J., COLLIER E., IMMERZEEL W.W. Contrasting meteorological drivers of the glacier mass balance between the Karakoram and central Himalaya. *Frontiers in Earth Science*, **7**, 107, **2019**.
20. BENN D.I., FOWLER A.C., HEWITT I., SEVESTRE H. A general theory of glacier surges. *Journal of Glaciology*, **65** (253), 701, **2019**.
21. WUITE J., ROTT H., HETZENECKER M., FLORICIOIU D., DE RYDT J., GUDMUNDSSON G.H., NAGLER T., KERN M. Evolution of surface velocities and ice discharge of Larsen B outlet glaciers from 1995 to 2013. *The Cryosphere*, **9** (3), 957, **2015**.
22. VIJAY S., KHAN S.A., KUSK A., SOLGAARD A.M., MOON T., BJØRK A. Resolving seasonal ice velocity of 45 Greenlandic glaciers with very high temporal details. *Geophysical Research Letters*, **46** (3), 1485, **2019**.
23. LIU G., GUO H., YUE H., PERSKI Z., YAN S., SONG R., FAN J., RUAN Z. Modified four-pass differential SAR interferometry for estimating mountain glacier surface velocity fields. *Remote Sensing Letters*, **7** (1), 1, **2016**.
24. MANDAL A., RAMANATHAN A., AZAM M.F., ANGCHUK T., SOHEB M., KUMAR N., POTTAKKAL J.G., VATSAL S., MISHRA S., SINGH V.B. Understanding the interrelationships among mass balance, meteorology, discharge and surface velocity on Chhota Shigri Glacier over 2002-2019 using in situ measurements. *Journal of Glaciology*, **66** (259), 727, **2020**.
25. DEHECQ A., GOURMELEN N., TROUVÉ E. Deriving large-scale glacier velocities from a complete satellite archive: Application to the Pamir-Karakoram-Himalaya. *Remote Sensing of Environment*, **162**, 55, **2015**.
26. FAHNSTOCK M., SCAMBOS T., MOON T., GARDNER A., HARAN T., KLINGER M. Rapid large-area mapping of ice flow using Landsat 8. *Remote Sensing of Environment*, **185**, 84, **2016**.
27. GARDNER A.S., MOHOLDT G., SCAMBOS T., FAHNSTOCK M., LIGTENBERG S., VAN DEN BROEKE M., NILSSON J. Increased West Antarctic and unchanged East Antarctic ice discharge over the last 7 years. *The Cryosphere*, **12** (2), 521, **2018**.
28. ZINNO I., MOSSUCCA L., ELEFANTE S., DE LUCA C., CASOLA V., TERZO O., CASU F., LANARI R. Cloud computing for earth surface deformation analysis via spaceborne radar imaging: A case study. *IEEE Transactions on Cloud Computing*, **4** (1), 104, **2015**.
29. HUANG L., LI Z. Comparison of SAR and optical data in deriving glacier velocity with feature tracking. *International Journal of Remote Sensing*, **32** (10), 2681, **2011**.

30. JOUGHIN I., SMITH B.E., HOWAT I. Greenland Ice Mapping Project: ice flow velocity variation at sub-monthly to decadal timescales. *The Cryosphere*, **12** (7), 2211, **2018**.
31. WATSON C.S., QUINCEY D. Glacier movement. *Geomorphological Techniques*; British Society for Geomorphology: London, UK, **2015**.
32. MOON T., JOUGHIN I., SMITH B., VAN DEN BROEKE M.R., VAN DE BERG W.J., NOËL B., USHER M. Distinct patterns of seasonal Greenland glacier velocity. *Geophysical research letters*, **41** (20), 7209, **2014**.
33. MOUGINOT J., RIGNOT E., SCHEUCHL B., FENTY I., KHAZENDAR A., MORLIGHEM M., BUZZI A., PADEN J. Fast retreat of Zachariæ Isstrøm, northeast Greenland. *Science*, **350** (6266), 1357, **2015**.
34. BUNCE C., CARR J.R., NIENOW P.W., ROSS N., KILLICK R. Ice front change of marine-terminating outlet glaciers in northwest and southeast Greenland during the 21st century. *Journal of Glaciology*, **64** (246), 523, **2018**.
35. FANG L., YE Z., SU S., KANG J., TONG X. Glacier surface motion estimation from SAR intensity images based on subpixel gradient correlation. *Sensors*, **20** (16), 4396, **2020**.
36. LEPRINCE S., BERTHIER E., AYOUB F., DELACOURT C., AVOUAC J.P. Monitoring earth surface dynamics with optical imagery. *Eos, Transactions American Geophysical Union*, **89** (1), 1, **2008**.
37. PAUL F., BOLCH T., BRIGGS K., KÄÄB A., MCMILLAN M., MCNABB R., NAGLER T., NUTH C., RASTNER P., STROZZI T., WUITE J. Error sources and guidelines for quality assessment of glacier area, elevation change, and velocity products derived from satellite data in the Glaciers\_cci project. *Remote Sensing of Environment*, **203**, 256, **2017**.
38. WANG R., LIU S., SHANGGUAN D., RADIĆ V., ZHANG Y. Spatial heterogeneity in glacier mass-balance sensitivity across High Mountain Asia. *Water*, **11** (4), 776, **2019**.
39. ØSTBY T.I., SCHULER T.V., HAGEN J.O., HOCK R., KOHLER J., REIJMER, C.H. Diagnosing the decline in climatic mass balance of glaciers in Svalbard over 1957–2014. *The Cryosphere*, **11** (1), 191, **2017**.
40. PRATAP B., DOBHAL D.P., BHAMBRI R., MEHTA M., TEWARI, V.C. Four decades of glacier mass balance observations in the Indian Himalaya. *Regional Environmental Change*, **16** (3), 643, **2016**.
41. LATIEF S.U., RASHID S., SINGH R. Impact analysis of climate change on Kolahoi Glacier in Liddar Valley, north-western Himalayas. *Arabian Journal of Geosciences*, **9** (18), 1, **2016**.
42. BAJRACHARYA S.R., MAHARJAN S.B., SHRESTHA F., GUO W., LIU S., IMMERZEEL W., SHRESTHA B. The glaciers of the Hindu Kush Himalayas: current status and observed changes from the 1980s to 2010. *International Journal of Water Resources Development*, **31** (2), 161, **2015**.
43. REN Y.Y., REN G.Y., SUN X.B., SHRESTHA A.B., YOU Q.L., ZHAN Y.J., Rajbhandari R., Zhang P.F., WEN K.M. Observed changes in surface air temperature and precipitation in the Hindu Kush Himalayan region over the last 100-plus years. *Advances in Climate Change Research*, **8** (3), 148, **2017**.
44. ASHRAF A. Upstream and downstream response of water resource regimes to climate change in the Indus River basin. *Arabian Journal of Geosciences*, **12** (16), 1, **2019**.
45. QURESHI M.A., YI C., XU X., LI Y. Glacier status during the period 1973-2014 in the Hunza Basin, Western Karakoram. *Quaternary International*, **444**, 125, **2017**.
46. AKRAM N., HAMID A. Climate change: A threat to the economic growth of Pakistan. *Progress in Development Studies*, **15** (1), 73, **2015**.
47. AMJAD D., KAUSAR S., WAQAR R., SARWAR F. Land cover change analysis and impacts of deforestation on the climate of District Mansehra, Pakistan. *Journal of Biodiversity Environmental Sciences*, **14** (6), 103, **2019**.
48. ZHOU Y., CHEN J., CHENG X. Glacier Velocity Changes in the Himalayas in Relation to Ice Mass Balance. *Remote Sensing*, **13** (19), 3825, **2021**.
49. AVIAN M., BAUER C., SCHLÖGL M., WIDHALM B., GUTJAHR K.H., PASTER M., HAUER C., FRIESSENBICHLER M., NEUREITER A., WEYSS G., FLÖDL P., SULZER W. The status of earth observation techniques in monitoring high mountain environments at the example of pasterze glacier, Austria: Data, methods, accuracies, processes, and scales. *Remote Sensing*, **12** (8), 1251, **2020**.
50. SABA S.B., ALI M., VAN DER MEIJDE M., VAN DER WERFF H. Co-seismic landslides automatic detection on regional scale with sub-pixel analysis of multi temporal high resolution optical images: Application to southwest of Port Au Prince, Haiti. *Journal of Himalayan earth sciences*, **50** (2), 74, **2017**.
51. NECSOIU M., ONACA A., WIGGINTON S., URDEA P. Rock glacier dynamics in Southern Carpathian Mountains from high-resolution optical and multi-temporal SAR satellite imagery. *Remote sensing of environment*, **177**, 21, **2016**.
52. FAHNESTOCK M., SCAMBOS T., MOON T., GARDNER A., HARAN T., KLINGER M. Rapid large-area mapping of ice flow using Landsat 8. *Remote Sensing of Environment*, **185**, 84, **2016**.
53. JAWAK S.D., KUMAR S., LUIS A.J., BARTANWALA M., TUMMALA S., PANDEY A.C. Evaluation of geospatial tools for generating accurate glacier velocity maps from optical remote sensing data. *Multidisciplinary Digital Publishing Institute Proceedings*, **2** (7), 341, **2018**.
54. AYOUB F., LEPRINCE S., KEENE L. User's guide to COSI-CORR co-registration of optically sensed images and correlation. *California Institute of Technology: Pasadena, CA, USA*, **38**, 49s, **2009**.
55. HUANG J., DENG K., FAN H., LEI S., YAN S., WANG L. An improved adaptive template size pixel-tracking method for monitoring large-gradient mining subsidence. *Journal of Sensors*, **2017**.
56. DING C., FENG G., LI Z., SHAN X., DU Y., WANG H. Spatio-temporal error sources analysis and accuracy improvement in landsat 8 image ground displacement measurements. *Remote Sensing*, **8** (11), 937, **2016**.
57. WU K., LIU S., XU J., ZHU Y., LIU Q., JIANG Z., WEI J. Spatiotemporal variability of surface velocities of monsoon temperate glaciers in the Kangri Karpo Mountains, southeastern Tibetan Plateau. *Journal of Glaciology*, **67** (261), 186, **2021**.
58. JEONG S., HOWAT I.M. Performance of Landsat 8 Operational Land Imager for mapping ice sheet velocity. *Remote Sensing of Environment*, **170**, 90, **2015**.
59. LEI W., ZONGLI J., SHIYIN L., DONGHUI S., YONG Z. Characteristic of glaciers' movement Along Karakoram highway. *Remote Sensing Technology and Application*, **34** (2), 412, **2019**.

60. LI Y., YAN S., LI Z., ZHOU H., ZHENG Y., LIU Q.Q. The flow state of South Inylchek glacier in the Tianshan Mountains in 2016: Extraction and analysis based on Landsat-8 OLI image. *J. Glaciol. Geocryol.*, **39** (6), 1281, **2017**.
61. SHUKLA A., GARG P.K. Spatio-temporal trends in the surface ice velocities of the central Himalayan glaciers, India. *Global and Planetary Change*, **190**, 103187, **2020**.
62. ANDREASSEN L.M., ELVEHØY H., KJØLLMOEN B., ENGESET R.V. Reanalysis of long-term series of glaciological and geodetic mass balance for 10 Norwegian glaciers. *The Cryosphere*, **10** (2), 535, **2016**.
63. SALERNO F., THAKURI S., TARTARI G., NUIMURA T., SUNAKO S., SAKAI A., FUJITA K. Debris-covered glacier anomaly? Morphological factors controlling changes in the mass balance, surface area, terminus position, and snow line altitude of Himalayan glaciers. *Earth and Planetary Science Letters*, **471**, 19, **2017**.
64. GAO H., ZOU X., WU J., ZHANG Y., DENG X., HUSSAIN S., WAZIR M.A., ZHU G. Post-20th century near-steady state of Batura Glacier: observational evidence of Karakoram Anomaly. *Scientific Reports*, **10** (1), 1, **2020**.
65. KUMAR V., SHUKLA T., MISHRA A., KUMAR A., MEHTA M. Chronology and climate sensitivity of the post-LGM glaciation in the Dunagiri valley, Dhauliganga basin, Central Himalaya, India. *Boreas*, **49** (3), 594, **2020**.
66. CANASSY P.D., RÖÖSLI C., WALTER F. Seasonal variations of glacier seismicity at the tongue of Rhonegletscher (Switzerland) with a focus on basal icequakes. *Journal of Glaciology*, **62** (231), 18, **2016**.
67. KRAAIJENBRINK P., MEIJER S.W., SHEA J.M., PELLICCIOTTI F., DE JONG S.M., IMMERZEEL W.W. Seasonal surface velocities of a Himalayan glacier derived by automated correlation of unmanned aerial vehicle imagery. *Annals of Glaciology*, **57** (71), 103, **2016**.
68. LEMOS A., SHEPHERD A., MCMILLAN M., HOGG A.E. Seasonal variations in the flow of land-terminating glaciers in Central-West Greenland using Sentinel-1 imagery. *Remote Sensing*, **10** (12), 1878, **2018**.
69. MANDAL A., RAMANATHAN A., AZAM M.F., ANGCHUK T., SOHEB M., KUMAR N., SINGH V.B. Understanding the interrelationships among mass balance, meteorology, discharge and surface velocity on Chhota Shigri Glacier over 2002-2019 using in situ measurements. *Journal of Glaciology*, **66** (259), 727, **2020**.
70. ALI S., KHAN G., HASSAN W., QURESHI J.A., BANO I. Assessment of glacier status and its controlling parameters from 1990 to 2018 of Hunza Basin, Western Karakorum. *Environmental Science and Pollution Research*, **28** (44), 63178, **2021**.
71. QURESHI J.A., KHAN G., ALI N., ALI S., BANO R., SAEED S., EHSAN M.A. Spatio-temporal Change of Glacier Surging and Glacier-dammed Lake Formation in Karakoram Pakistan. *Earth Systems and Environment*, **6** (1), 249, **2022**.
72. ABBAS GILANY S.N., IQBAL J., HUSSAIN E. Geospatial analysis and simulation of glacial lake outburst flood hazard in Hunza and Shyok basins of upper Indus basin. *The Cryosphere Discussions*, **1**, **2020**.
73. SHAFIQUE M., FAIZ B., BACHA A.S., ULLAH S. Evaluating glacier dynamics using temporal remote sensing images: a case study of Hunza Valley, northern Pakistan. *Environmental earth sciences*, **77** (5), 1, **2018**.
74. TALOOR A.K., KOTHYARI G.C., MANHAS D.S., BISHT H., MEHTA P., SHARMA M., MAHAJAN S., ROY S., SINGH A.K., ALI S. Spatio-temporal changes in the Machoi glacier Zaskar Himalaya India using geospatial technology. *Quaternary Science Advances*, **4**, 100031, **2021**.
75. KUMAR V., MEHTA M., SHUKLA T. Spatially resolved estimates of glacial retreat and lake changes from Gepang Gath Glacier, Chandra Basin, Western Himalaya, India. *Journal of the Geological Society of India*, **97** (5), 520, **2021**.
76. SAHA S.K., SENTHIL KUMAR A. Northwest Himalayan Ecosystems: Issues, Challenges and Role of Geospatial Techniques. In *Remote Sensing of Northwest Himalayan Ecosystems* (pp. 3-14). Springer, Singapore, **2019**.
77. HAZRA P., KRISHNA A.P. Spatio-temporal and surface elevation change assessment of glaciers of Sikkim Himalaya (India) across different size classes using geospatial techniques. *Environmental Earth Sciences*, **78** (14), 1, **2019**.
78. GARG V., KUDEKAR A.R., THAKUR P.K., NIKAM B.R., AGGARWAL S.P., CHAUHAN P. Glacier change studies under changing climate using geospatial tools and techniques. *Journal of the Indian Society of Remote Sensing*, **49** (10), 2387, **2021**.
79. SINGH D.K., THAKUR P.K., NAITHANI B.P., DHOTE P.R. Spatio-temporal analysis of glacier surface velocity in dhauliganga basin using geo-spatial techniques. *Environmental Earth Sciences*, **80** (1), 1, **2021**.
80. SAHU R., GUPTA R.D. Surface velocity dynamics of Samudra Tapu Glacier, India from 2013 to 2017 using Landsat-8 data. *ISPRS Annals of the Photogrammetry, Remote Sensing and Spatial Information Sciences*, **4**, 75, **2019**.
81. GADDAM V.K., BODDAPATI R., KUMAR T., KULKARNI A.V., BJORNSSON H. Application of "OTSU" – an image segmentation method for differentiation of snow and ice regions of glaciers and assessment of mass budget in Chandra basin, Western Himalaya using Remote Sensing and GIS techniques. *Environmental Monitoring and Assessment*, **194** (5), 1, **2022**.
82. RASHID I., MAJEED U., JAN A., GLASSER N.F. The January 2018 to September 2019 surge of Shisper Glacier, Pakistan, detected from remote sensing observations. *Geomorphology*, **351**, 106957, **2020**.
83. BHUSHAN S., SYED T.H., ARENDT A.A., KULKARNI A.V., SINHA D. Assessing controls on mass budget and surface velocity variations of glaciers in Western Himalaya. *Scientific reports*, **8** (1), 1, **2018**.
84. MAJEED U., RASHID I. Evaluating glacier surges in Karakoram region using earth observation data. *Data in Brief*, **30**, 105394, **2020**.
85. MURTAZA K.O., DAR R.A., PAUL O.J., BHAT N.A., ROMSHOO S.A. Glacial geomorphology and recent glacial recession of the Harmukh Range, NW Himalaya. *Quaternary International*, **575**, 236, **2021**.
86. KALITA H., GHOSH T., RANI M., RAWAT J.S., SINGH R.K., SINGH S.K., KUMAR P. Retreating Glacier Dynamics Over the Last Quarter of a Century in Uttarakhand Region Using Optical Sensor Time Series Data. In *Remote Sensing and GIScience* (pp. 75-93). Springer, Cham, **2021**.
87. LIU Y., WANG N., ZHANG J., WANG L. Climate change and its impacts on mountain glaciers during 1960-2017 in western China. *Journal of Arid Land*, **11** (4), 537, **2019**.
88. TIWARI A., KUMAR K., PATLEY M., SHARMA J. Application of Geospatial Techniques for Monitoring the Cryospheric Elements of Glacier System in Indian

- Himalayan Region (IHR). In *Water, Cryosphere, and Climate Change in the Himalayas* (pp. 1-18). Springer, Cham, **2021**.
89. SHAFIQUE M., FAIZ B., BACHA A. Evaluating glacier dynamics using temporal remote sensing images: a case study of hunza valley, northern pakistan. *International Archives of the Photogrammetry, Remote Sensing & Spatial Information Sciences*, **2019**.
90. SIVALINGAM S., MURUGESAN G.P., DHULIPALA K., KULKARNI A.V., PANDIT A. Essential study of Karakoram glacier velocity products extracted using various techniques. *Geocarto International*, **1**, **2021**.
91. MENG Q., CHEN X., HUANG X., HUANG Y., PENG Y., ZHANG Y., ZHEN J. Monitoring glacier terminus and surface velocity changes over different time scales using massive imagery analysis and offset tracking at the Hoh Xil World Heritage Site, Qinghai-Tibet Plateau. *International Journal of Applied Earth Observation and Geoinformation*, **112**, 102913, **2022**.
92. SINGH D.K., THAKUR P.K., NAITHANI B.P., KAUSHIK S. Temporal monitoring of glacier change in dhauliganga basin, kumaun himalaya using geo-spatial techniques. *ISPRS Annals of Photogrammetry, Remote Sensing & Spatial Information Sciences*, **4** (5), **2018**.
93. KUMAR V., SHUKLA T., MEHTA M., DOBHAL D.P., BISHT M.P.S., NAUTIYAL S. Glacier changes and associated climate drivers for the last three decades, Nanda Devi region, Central Himalaya, India. *Quaternary International*, **575**, 213, **2021**.
94. DUTTA S., RAMANATHAN A.L. Estimation of Deglaciation through Remote Sensing Techniques in Chandra-Bhaga Basin, Western Himalaya. *Journal of Climate Change*, **7** (1), 79, **2021**.
95. SATTAR A., GOSWAMI A., KULKARNI A.V., DAS P. Glacier-surface velocity derived ice volume and retreat assessment in the dhauliganga basin, central himalaya – A remote sensing and modeling based approach. *Frontiers in Earth Science*, **7**, 105, **2019**.